PROCEEDINGS OF

INNOVATION AND TECHNOLOGY EXPOSITION 2018 (InTEX18) CONFERENCE

Digitalising Sarawak Translational Research

17-18 July 2018
Pullman Kuching

TABLE OF CONTENTS

Biodiversity & Environmental Conservation **(BEC)** Page

Information, Communication & Creative Technology **(ICCT)** Page

Sustainable Community Transformation **(SCT)** Page

Biodiversity & Environmental Conservation
(BEC)

INNOVATION TECHNOLOGY EXPO
(INTEX) 2018 CONFERENCE
Kuching, Sarawak, Malaysia, July 17-18, 2018

BEC-2018-01

Expression Patterns of the Human Ribosomal Protein Genes *eL14* and *uS19* in Colon Cancer is Dependent on the Type and Stage of the Cancer Cell

Edmund Ui-Hang Sim[1,*], Selvamalar Mutsamy[1] and Zy-Ying Teh[1]

[1] Faculty of Resource Science and Technology, Universiti Malaysia Sarawak, 94300 Kota Samarahan, Sarawak, MALAYSIA
* (E-mail: uhsim@unimas.my)

Association of ribosomal protein genes with cancer of the colon and rectum is widely known but not in depth. More importantly, the behaviors of these genes in different types and stages of the cancer are yet to be fully demonstrated. Herein we report the study of two ribosomal protein (RP) genes in cell lines derived from different sites and stages of colon cancer. Specifically, we analyzed the expression pattern of *eL14* and *uS19* in HCT116 and SW480 cell lines. These two RP genes, although associated with a wide variety of cancer types [1-5], are poorly or have not been studied in colorectal cancer. HCT116 is a poorly differentiated colorectal carcinoma cell line derived from the metastatic cells of the ascending colon, while SW480 is a moderately differentiated non-metastatic colorectal adenocarcinoma cell line from the descending colon [6]. Semi-quantitative reverse transcription – polymerase chain reaction (RT-PCR) approach together with Students' t-test validation were used to evaluation expression level.

Our results showed that *eL14* expression is detected in the colorectal carcinoma cell line (HCT116) but not in the colorectal carcinoma cell line (SW480) (Figure 1), while expression of *uS19* was present in both HCT116 and SW480 cell lines (Figure 2). For uS19, expression in HCT116 was significantly higher compared to SW480 (*p*-value of 0.026).

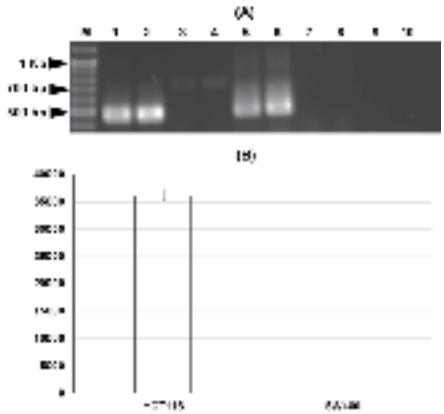

Figure 1. Expression pattern of *eL14* in HCT116 and SW480 cell lines. (A), Electrophoretic results of RT-PCR assay (Lane M: DNA Ladder, lanes 1 and 2: *GAPDH* amplicons in HCT116, lanes 3 and 4: *eL14* amplicons in HCT116, lanes 5 and 6: *GAPDH* amplicons in SW480, lanes 7 and 8: *eL14* amplicons in SW480, and lanes 9 and 10 are negative controls of *eL14* test for HCT116 and SW480 respectively. (B), Column chart of mean band intensity value with error bar. The y-axis represents band intensity values, and the x-axis is the type of cell lines.

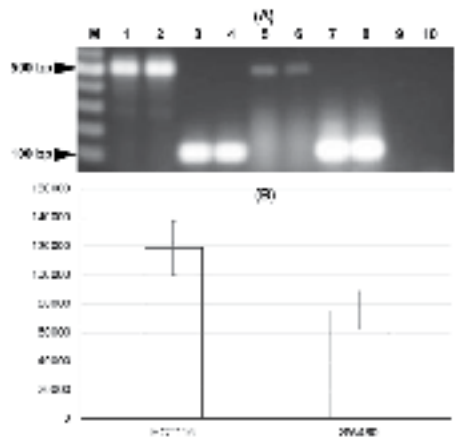

Figure 2. Expression pattern of *uS19* in HCT116 and SW480 cell lines. (A), Electrophoretic results of RT-PCR assay (Lanes 1 and 2: *GAPDH* amplicons in SW480, lanes 3 and 4: *uS19* amplicons in SW480, lanes 5 and 6: *GAPDH* amplicons in HCT116, lanes 7 and 8: *uS19* amplicons in HCT116, and lanes 9 and 10 are negative controls of *uS19* test for HCT116 and SW480 respectively. (B), Column chart of mean band intensity value with error bar. The y-axis represents band intensity values, and the x-axis is the types of cell line.

Our findings on *eL14* and *uS19* suggest a marked or elevated expression in metastatic rather than non-metastatic cells. Specifically, *eL14* and *uS19* were highly expressed in the poorly differentiated metastatic colorectal carcinoma cell line, HCT116. In the moderately differentiated colorectal adenocarcinoma non-metastatic cell line, SW480, *eL14* was not detected, and *uS19* was expressed but at a significantly lower level compared to HCT116. Although differential expression of up to 18 RPs in tumour cell lines of the same origin but different metastatic abilities has been reported [7], our study is the first to demonstrate this behavior for *eL14* and *uS19* in colorectal malignancy. This implies biomarker potential for these two RP genes in carcinogenesis of the colorectum. Nonetheless, evaluation of their protein levels in the tested cell lines is still required to verify our suspicion.

Acknowledgment: This research is funded by the Fundamental Research Grant Scheme [FRGS/ST03(02)/1299/2015(16)].

References:

[1] Huang, X.P., Zhao, C.X., Li, Q.J., et al. (2006). Alteration of RPL14 in squamous cell carcinomas and preneoplastic lesions of the esophagus. *Gene*, 366(1): 161-168.

[2] Yoon, S.Y., Kim, J., Oh, J., et al. (2006). Gene expression profiling of human HBV- and/or HCV-associated hepatocellular carcinoma cells using sequence tags. *International Journal of Oncology*, 29: 315-327.

[3] Lai, M., Xu, J. (2007). Ribosomal proteins and colorectal cancer. *Genomics*, 8: 43-49.

[4] Fang, W., Li, X., Jiang, Q., et al. (2008). Transcriptional patterns, biomarkers and pathways characterizing nasopharyngeal carcinoma of Southern China. *Journal of Translational Medicine*, 6(32): 1-13.

[5] Sim, E.U.H., Chee, C.S.M., Vasudevan, L., Ng, K.L., Chan, S.L.L. (2018). Selective differential expression of the ribosomal protein genes eL14 and uS19 in a well-differentiated epithelial cell line of nasopharyngeal carcinoma. *Malaysian Applied Biology*, 47(1): 247–253.

[6] Niu, N., Zhang, J., Huang, T., et al. (2012). IgG expression in human colorectal cancer and its relationship to cancer behaviors. *PLoS One*, 7(11): 247362.

[7] Kreunin, P., Yoo, C., Urquidi, V., Lubman, D.M., Goodison, S. (2007). Differential expression of ribosomal proteins in a human model identified by coupling 2-D liquid chromatography and mass spectrometry. *Cancer Genomics Proteomics*, 4(5): 329-339.

INNOVATION TECHNOLOGY EXPO
(INTEX) 2018 CONFERENCE
Kuching, Sarawak, Malaysia, July 17-18, 2018

BEC-2018-02

Perceived Susceptibility and Severity of Diarrhoea, Nasopharyngeal Cancer and Human Immunodeficiency Virus Infection

Yuwana Podin[1,*], Su-Hie Ting[2], Collin Jerome[2] and Sharifah S.W. Ahmad[3]

[1] Institute of Health and Community Medicine, Universiti Malaysia Sarawak, MALAYSIA.
[2] Faculty of Language and Communication, Universiti Malaysia Sarawak, MALAYSIA.
[3] Faculty of Social Sciences and Humanities, Universiti Malaysia Sarawak, MALAYSIA.
* (E-mail: pyuwana@unimas.my)

Perceived risk and efficacy beliefs are motivators of change in health behaviours to minimise risk from developing a disease. Nasopharyngeal cancer (NPC) refers to nose and throat cancer where it is among the top five cancers in Malaysia based on the latest National Cancer Registry records on disease incidence. In addition, Malaysian men rank second and Malaysian women rank first for NPC in the world [1]. To date, research on public perceptions of cancer have shown some awareness of cancer but not specifically on NPC and thus far, studies on NPC in Malaysia focus mainly on the clinical perspectives of the disease.

In order to obtain a better understanding of perceived risk and severity of NPC, it is necessary to study public perceptions in the context of other diseases, particularly infectious diseases of different severity such as diarrhoea and human immunodeficiency virus (HIV) infection. The present study examined perceived susceptibility and severity of diarrhoea, NPC and HIV infection using the risk perception attitude framework as shown in Figure 1 [2, 3].

In the preliminary study conducted on 10 participants who do not have nasopharyngeal cancer and HIV diseases, participants were given three questionnaires for the three diseases on susceptibility, severity, response efficacy and self-efficacy. The data were analysed by computing frequency counts and mean scores for each item.

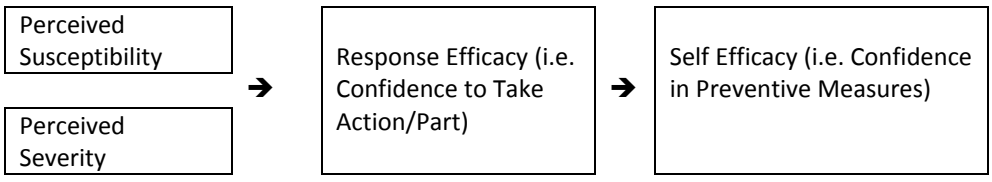

Figure 1. Framework showing the combination of perceived susceptibility and severity, leading to response efficacy and self-efficacy [2,3]

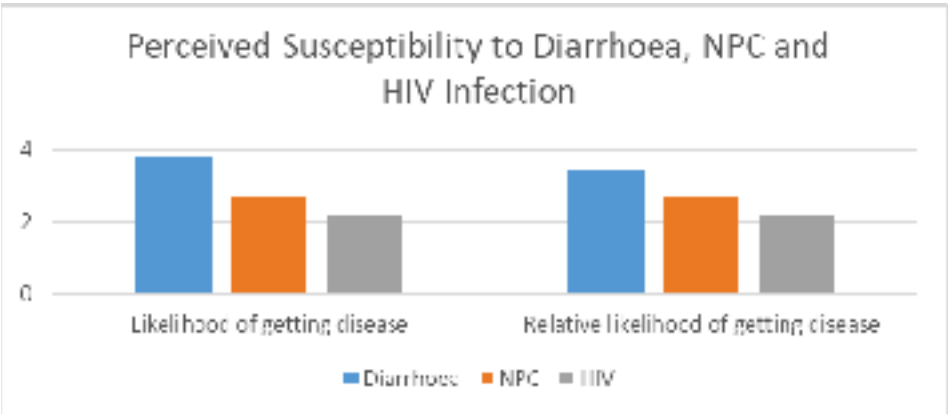

Figure 2. Perceived susceptibility of respondents to diarrhoea, NPC, and HIV infection

Results revealed that perceived susceptibility to diarrhoea was the highest and HIV was the lowest (Figure 2). However, the severity of HIV was the highest and diarrhoea was considered not a serious disease. Response efficacy and self-efficacy beliefs were similar for the three diseases, with the participants reporting confidence to take action to reduce risk from the disease and confidence in the effectiveness of the measures to reduce risk. The classification of the participants into four groups based on the risk perception attitude framework shows that all except one were in the responsive group (high risk, strong efficacy); they exhibit high risk perceptions and strong efficacy beliefs, which means they are motivated to act and engage extensively in self-protective behaviours. This was true for all three diseases studied, irrespective of the severity of disease (HIV and NPC being more severe) and infectiousness of disease (diarrhoea and HIV).

In conclusion, the study revealed that the participants' health beliefs towards infectious or non-infectious diseases are consistent where they exhibited responsive attitudes towards diarrhoea, NPC and HIV. The individuals generally have high risk perceptions and strong efficacy beliefs. These findings are expected to help inform public health awareness programmes with disease-specific recommendations. An area for further research is to investigate the health beliefs of people who have experienced the diseases or carers who are in close contact with them.

Acknowledgment: The authors would like to express appreciation for the support of the Transdisciplinary Grant Scheme [Project Number = F09/TRGS/1519/2016].

References:

[1] Omar, Z. A., & Tamin, N. S. I. (2007). *National cancer registry report: Malaysia cancer statistics – data and figure 2007*. Putrajaya, Malaysia: Ministry of Health Malaysia.

[2] Rimal, R. N., & Real, K. (2003). Perceived risk and efficacy beliefs as motivators of change. *Human Communication Research*, *29*(3), 370-399.

[3] Rimal, R. N., Böse, K., Brown, J., Mkandawire, G., & Folda, L. (2009). Extending the purview of the risk perception attitude framework: findings from HIV/AIDS prevention research in Malawi. *Health Communication*, *24*(3), 210-218.

INNOVATION TECHNOLOGY EXPO
(INTEX) 2018 CONFERENCE
Kuching, Sarawak, Malaysia, July 17-18, 2018

BEC-2018-03

Evaluation of Ubi Gajah for Fuel Bioethanol via Hydrolysis and Fermentation

A. A. Saleh[1,*], A. N. R. Reddy[1,2], N. A. Nadia[1], D.K. Charyulu[2] and S. Hamdan[1]

[1] Department of Mechanical and Manufacturing Engineering, Faculty of Engineering, Universiti Malaysia Sarawak, 94300 Kota Samarahan, Sarawak, Malaysia.
[2] Department of Mechanical Engineering, Malla Reddy college of Engineering & Technology, Secunderabad - 500100, Telangana, India.
*(E-mail: aasaleh@unimas.my)

Energy is one of the most fundamental essential needs of life[1]. This research focuses on evaluation of diesel engine performance and gas emission fuelled with bioethanol - diesel blends (BDB). Bioethanol was produced using both Ubi Gajah peels and pulp by acid hydrolysis. Naturally grown raw Ubi Gajah was obtained from a local village, Jalan Jambusan Bau, located in Sarawak, Malaysia.

The Ubi Gajah pulp and peels were separated manually, chopped into smaller pieces and were blended using a heavy duty professional electric blender (OmniBlend V, imbaco, Australia). The samples were divided equally and kept in different beakers for further experimentation. Acid pre-treatment was carried out by adding H_2SO_4 of 5% v/v, 10% v/v and 15% v/v into the substrate samples as prepared. The mixtures were autoclaved for 3 hrs and the hydrolysed solutions were then filtered, while, the glucose concentration in each sample solution was measured using pocket refractometers. The Figures 1(a) and 1(b) shows autoclaved substrate solutions of three different concentrations after 3hrs of hydrolysis as well as turned to reddish brown. Higher the concentration of acid used to soak the substrate, the darker the colour of the solution obtained. After filtration process, the solutions are free of impurities.

Figure 1. Solutions of Ubi Gajah (a) Before hydrolysed (b) After Hydrolysed and filtered using 5%, 10% and 15 % v/v H_2SO_4.

It is found that acid concentration is greatly affecting the glucose produced. As glucose concentration increases, more ethanol can be produced from fermentation process. This has enhanced the production of bioethanol from 83.22 g/L to 109.45 g/L and 156.65 g/L at the end of the fermentation period. The density determined for both Ubi Gajah peels and pulp samples reveals that the peels sample is denser than pulp sample but

both samples' temperatures are differing. Ethanol sample generally has a density that is easily affected by the temperature and the pressure of surroundings. Based on the gas emission test results, E-diesel blends emitted lower SO_2 and NO_X. The emission of NO_X blends decreased with ethanol content. The increasing oxygen content from the ethanol can promote the formation of NOx but the maximum gas temperature is the most important factor of NOx formation. The decreased gas temperature caused by higher latent heat of vaporization of ethanol can reduce the NOx emission [2].

Table 1: Diesel Engine Performance indicators fuelled with bioethanol blends.

Engine Performance Indicator	Diesel	5% BDB	10% BDB	15% BDB	20% BDB
Torque (Nm)	36	36	36	36	36
Fuel Consumption Rate (ml/s)	0.1009	0.104	0.1067	0.1079	0.1089
Engine Power (kW)	0.585	0.5527	0.5053	0.4894	0.4739
Specific Fuel Consumption (ml/kW)	34.188	36.186	39.5804	40.8664	42.203
Brake Horsepower (kW)	4.2675	4.113	4.047	4.0282	4.0093
Horsepower (kW)	57.80	57.80	57.80	57.80	57.80
Mechanical Efficiency (%)	92.6268	92.8841	92.9983	93.0308	93.0635

The performance results of diesel engine were presented in Table 1. In terms of mechanical efficiency, diesel blends are less efficient compared to BDB fuel. Mechanical efficiency was increasing when more ethanol was added to diesel fuel. However, ethanol-diesel blends decreased the power of diesel engine without modification. This will lead to an increase in the specific fuel consumption [3]. Thus, the higher the ethanol content, the greater the fuel consumption will be. In conjunction to the addition of ethanol to diesel, brake horsepower will be decreased with the volume of ethanol added [4]. The experimental results obtained indicates that Ubi Gajah is a suitable alternative feedstock source for bioethanol production. Even though the blending has better mechanical efficiency and cleaner gas emission, fuel consumption rate is high which is ineffectual.

Acknowledgment: The authors would like to acknowledge Universiti Malaysia Sarawak for providing the technical and financial assistance during this work under the grant F02/SpFRGS/1538/2017.

References:

[1] S. Shafiee and E. Topal, "When will fossil fuel reserves be diminished?," *Energy Policy*, vol. 37, no. 1, pp. 181–189, 2009.

[2] J. Lei, Y. Bi, and L. Shen, "Performance and Emission Characteristics of Diesel Engine Fueled with Ethanol-Diesel Blends in Different Altitude Regions," *J. Biomed. Biotechnol.*, vol. 2011, pp. 1–10, 2011.

[3] A. Matuszewska, M. Odziemkowska, and J. Czarnocka, "Properties of bioethanol - diesel oil mixtures," *Mater. Process. energy Commun. Curr. Res. Technol. Dev.*, pp. 352–359, 2013.

[4] S. Gomasta and S. K. Mahla, "An Experimental Investigation of Ethanol Blended Diesel Fuel on Engine Performance and Emission of a Diesel Engine," *Int. J. Emerg. Technol.*, vol. 3, no. 1, pp. 74–79, 2012.

INNOVATION TECHNOLOGY EXPO
(INTEX) 2018 CONFERENCE
Kuching, Sarawak, Malaysia, July 17-18, 2018

BEC-2018-04

Effect of Nanoclay on the Thermal Properties of Silane Treated Jute/Polyethylene Nanocomposites

Md. Faruk Hossen[1, 2,*], Sinin Hamdan[1] and Md. Rezaur Rahman[1]

[1] Faculty of Engineering, Universiti Malaysia Sarawak, 94300 Kota Samarahan, Sarawak, Malaysia
[2] Faculty of Science, University of Rajshahi, Rajshahi-6205, Bangladesh
[*] (Email: fhossen.chem@gmail.com)

Currently, jute fiber reinforced polymer composites have been widely used in various industries [1]. Due to the hydrophilic nature of fiber and nanoclay, they exhibited poor interfacial interaction to hydrophobic polymer matrix. In order to enhance the interfacial interaction among fiber, polymer, and nanofillers, the chemically treated jute (with 3-isocyanatopropyltriethoxy silane) and organically modified five types of montmorillonite (MMT) nanoclay (MMT-1.28E, MMT-1.30E, MMT-1.31PS, MMT-1.34TCN, and MMT-1.44P) were used for the manufacturing of nanocomposites in this study. It had been reported by the author that the silane treated jute with organically modified 2 wt% of MMT nanoclay loaded jute polyethylene nanocomposite showed a substantial improvement in mechanical properties [2]. The thermal properties of silane treated jute/polyethylene/MMT nanoclay nanocomposites had not been reported yet. Therefore, in this study, the effects of nanoclay on the improvement of thermal properties of silane treated jute fiber reinforced polyethylene/clay nanocomposites have been investigated. The thermogravimetric analysis (TGA) was used to study the thermal behaviour of the 15 wt% fiber loaded composites reinforced silane treated jute with and without different types of nanoclay are shown in Figure 1.

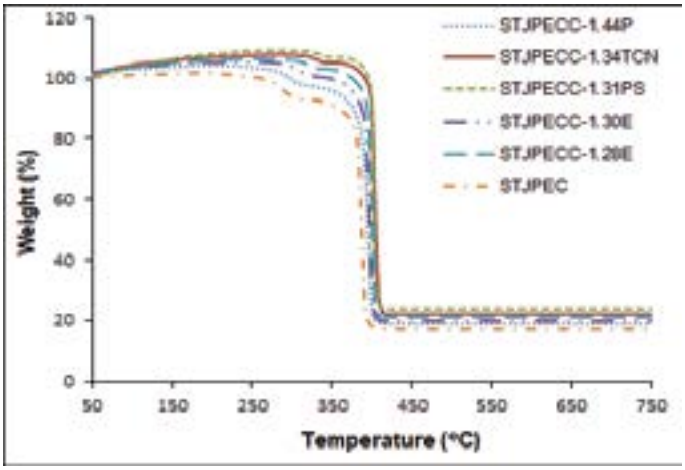

Figure 1. TGA Curves for 15 wt% fiber loaded STJPEC, STJPECC-1.28E, STJPECC-1.30E, STJPECC-1.31PS, STJPECC-1.34TCN, and STJPECC-1.44P.

The maximum rate of decomposition patterns of the prepared composites was observed in two stages. The first stage was observed within 288-330°C attributed to the degradation of lignin and hemicellulose. The second stage appeared within 372-388°C indicating the degradation of cellulose and other cellulosic matters from the fiber which lead to the char formation [3]. The addition of nanoclay led to a positive effect on thermal degradation which is indicated by higher thermal stability. The decomposition peaks of MMT incorporated composites (STJPECC) showed higher value than without nanoclay composite (STJPEC). The highest decomposition was observed for MMT-1.31PS nanoclay filled nanocomposite (STJPECC-1.31PS) among five nanoclay used in this research. This might be due to the MMT with greater carbon number of modifier that increases the hydrophobicity and finally increased interfacial adhesion between polymer matrix and MMT [4]. In contrast, MMT with less carbon number of modifier are poorly dispersed inside the composite system which cause air bubble and agglomerations [5]. It had also been reported earlier that the increase in thermal stability for chemically treated jute/polyethylene/clay nanocomposites [6, 7]. The above observations support the improved interfacial interaction between jute, polymer matrix and nanoclay due to addition of nanofiller.

The findings of this study provide evidence that the interfacial interaction among fiber, polymer matrix and nanoclay has become more favorable due to the carbon number of nanoclay modifier into the composite system. This work will help to develop the performance of nanocomposites in structural applications.

Acknowledgment: The authors would like to thankfully acknowledge the financial support provided by Universiti Malaysia Sarawak under the DPD Research Grant F02/DPD/1598/2017.

References:

[1] Botaro VR, Siqueira G, Megiatto JD. and Frollini E. Sisal fibers treated with NaOH and benzophenonetetracarboxylic dianhydride as reinforcement of phenolic matrix. *Journal of Applied Polymer Science,* vol. 115, no. 1, pp. 269-276, 2010.

[2] Hossen MF, Hamdan S, and Rahman MR. Improved mechanical properties of silane treated jute/polyethylene/clay nanocomposites. *Malaysian Applied Biollogy,* vol. 47, no. 1, pp. 209-215, 2018.

[3] Raghavendra G, Ojha S, Acharya SK, and Pal SK. Jute fiber reinforced epoxy composites and comparison with the glass and neat epoxy composites. *Journal of Composite Materials,* vol. 48, no. 20, pp. 2537-2547, 2014.

[4] Lan T and Pinnavaia TJ. Clay-reinforced epoxy nanocomposites. *Chemistry of Materials,* vol. 6, no. 12, pp. 2216-2219, 1994.

[5] Haq M, Burgueno R, Mohanty AK, and Misra M. Processing techniques for bio-based unsaturated-polyester/clay nanocomposites: Tensile properties, efficiency, and limits. *Composites Part A: Applied Science and Manufacturing,* vol. 40, no. 4, pp. 394-403, 2009.

[6] Hossen MF, Hamdan S, Rahman MR, Islam MS, Liew FK, Lai JCH, and Rahman MM. Improved thermal properties of jute fiber-reinforced polyethylene nanocomposites. *Polymer Composites,* DOI 10.1002/pc.23691, 2015.

[7] Hossen MF, Hamdan S, Rahman MR, Islam MS, Rahman MM, Kiew LF, and Lai JCH. Effect of clay content on the morphological, thermo-mechanical and chemical resistance properties of propionic anhydride treated jute fiber/polyethylene/nanoclay nanocomposites. *Measurement,* vol. 90, pp. 404-411, 2016.

BEC-2018-05

INNOVATION TECHNOLOGY EXPO
(INTEX) 2018 CONFERENCE
Kuching, Sarawak, Malaysia, July 17-18, 2018

Characteristics of Artificial Lightweight Aggregates Produced from Palm Oil Fuel Ash and Fly Ash Using Cold-Bonding

L.Y. Jong[1,*], D.C.L. Teo[1] and M.A. Mannan[1]

[1] Faculty of Engineering, Universiti Malaysia Sarawak
[*] (Email: xnykira90@gmail.com)

This paper is intended to determine the characteristics of artificial lightweight aggregate (ALWA) made from industrial solid wastes such as Palm Oil Fuel Ash (POFA) and Fly Ash (FA) using cold bonding method. Nowadays, the growth of industries is increasing due to the rapid change in population, and as a result, a large amount of industrial solid wastes is generated and dumped in landfills without any profitable return. FA and POFA are industrial waste materials commonly found in Malaysia. FA has been used in the construction of some structures which includes Petronas Twin Towers, the Second Malaysia-Singapore Causeway [1], and roller compacted concrete dam [2]. However, the usage of FA is still not widely applied in construction industry. In Malaysia, approximately 2.7 million tonnes of POFA is estimated to be discharged in year 2014 [3]. In particular, Sarawak is 2nd largest palm planted area in Malaysia, with an estimated 0.6 million tonnes of POFA generated in year 2014 alone [3]. As the quantity of POFA discharged is expected to increase annually, the allocation of transportation costs and landfills for the disposal of POFA are not effective ways to manage this waste as it may lead to environmental problems in the future (see Figure 1).

Figure 1. POFA Discharged from Mill and Dumped in Landfill

FA, POFA, of sodium hydroxide (NaOH) and sodium silicate (Na_2SiO_3) were used in this study. All the materials were obtained locally. The combination of NaOH and

industrial grade Na_2SiO_3 were used as the binder in this study. The raw materials, POFA and FA were mixed homogeneously in a tray. The percentage of POFA to FA used in this study was 80% and 20%, respectively. The molarities of sodium hydroxide used were 8M and 10M and ratio of sodium silicate to sodium hydroxide used was 1:1 by volume in this study. Pelletisation was carried out in a pelletiser disc of 570 mm diameter, with an inclined angle of 74° and a speed of 55 rpm. After production, these pellets were cured in a sealed container for 28 days. At the end of the curing period, the properties of aggregate were analysed, which includes particle density, bulk density, water absorption, and crushing strength.

All the aggregates are satisfied the requirements as lightweight aggregates, in which particle density of aggregate not exceeding 2000 kg/m^3 or a loose bulk density of aggregate not exceeding 1200 kg/m^3. The results show that greater molarity of NaOH would give higher bulk density and particle density of POFA FA aggregates. Increasing in concentration of NaOH would reduce the water absorption of POFA FA aggregates. The crushing strength of all aggregates are increasing from 3 days to 28 days regardless of NaOH concentration. Aggregate with higher molarity of NaOH (10M) shows a better crushing strength as compared to aggregate with lower molarity of NaOH (8M).

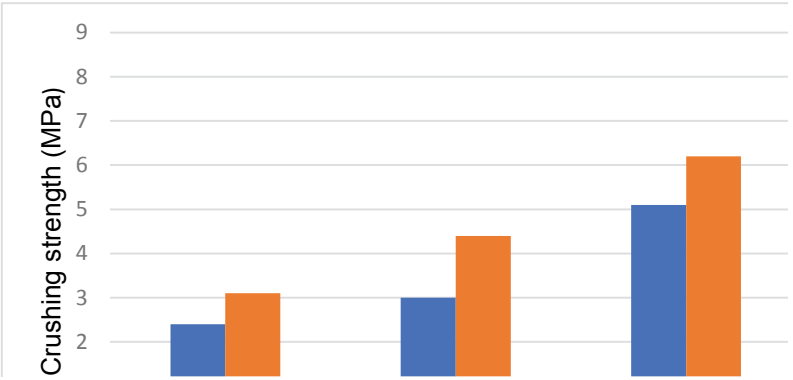

Figure 2. The Strength Development of POFA FA Aggregates for Different Molarity of NaOH

Acknowledgment: This project was funded by Special Grant Scheme (F02/SpFRGS/1539/2017) rendered by the Universiti Malaysia Sarawak.

References:

[1] Kidav, E. U., Soo, T. P., Sirivivatnanon, V., and Khatri, R. (2001). Advances in Malaysian Fly Ash Concrete Technology. *Special Publication*, 199, 343-360.

[2] Zulkifli, A. R., Hamid, A. R. A., Arshad, M. F., and Ahmad, J. (2015). Construction of Roller Compacted Concrete Dam in Malaysia: A Case Study at Batu Hampar Dam. *In Proceedings of the International Civil and Infrastructure Engineering Conference 2014*, 727-739.

[3] Malaysian Palm Oil Board (MPOB). (2017). Overview of the Malaysian Oil Palm Industry. Available from: http://bepi.mpob.gov.my/images/overview/Overview_of_Industry_2017.pdf

INNOVATION TECHNOLOGY EXPO
(INTEX) 2018 CONFERENCE
Kuching, Sarawak, Malaysia, July 17-18, 2018

BEC-2018-06

A Resultant Force Analysis of Current Design for Thresher Operation in Palm Oil Mill Industry

Shanti Faridah Salleh[1,*], Shareena Saree[1], Khairuddin Sanaullah[1], Afrasyab Khan[1], Robiah Yunus[1], Marini Sawawi[1], Nordiana Rajaee[1], Norzafirah Azriah Mohd Fadzli[1] and Mohammed Haji Alhaji[1]

[1] Faculty of Engineering, Universiti Malaysia Sarawak
[*] (Email:sshanti@unimas.my)

The palm oil mill industry is a vital aspect of the agricultural sector that has contributed immensely to the world economic growth. The development of this sector has been on downward trend recently due to world economic recession, the technological input for oil extraction is the factor that contributes to this production setback in the industry [1]. Therefore, there is the need to develop an advanced technology that will enable a spontaneous increase in the Oil Extraction Rate (OER).

This study is aimed at the development of technological mode of operation for the thresher unit which has seldom been neglected over the years. A computational numerical analysis has been selected for this study with the simulation of applied force of stickiness together with the necessary centrifugal force from within and outside of the thresher (in Figure 1).

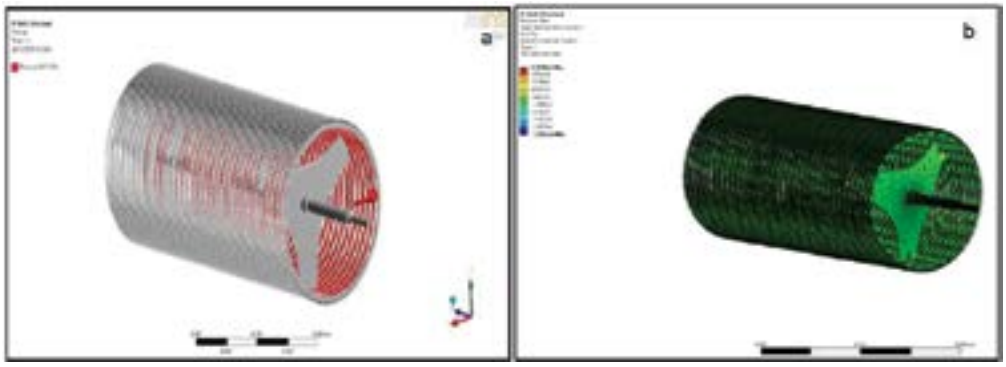

Figure 1. (a) The Total Force acted at the whole body of the Thresher Drum (b) Resolution of Forces across the body of thresher after the Simulation Study.

The thresher design has been drawn using Solid Work® software in a 3D Dimension. The mesh geometers of the thresher obtained have been imported into the ANSYS® 14.0 software. The thresher shape domains were drawn based on Serian Palm Oil mill "Technical drawing (Drawing Number: SEPOM/TS/11)". Similarly, a finite element for the thresher to study the two varieties of the palm fruit: Dura and Tenera has been obtained. In order to

obtained the resultant force, the effects of the type of fruits, material of thresher, loading within and outside of the thresher and rotational velocity have been studied [2].

The resistance force has been obtained through the calculation all the loads obtains from the thresher body as well as from its revolution per minute (rpm). The calculation of the impact of the opposite force either same or higher was done for both inside and outside of the thresher and has proposed to ascertain gravity of forces of the fruit spikelet on the thresher. The result from this study will be useful in the design of an efficient process for achieving high oil extraction rate in the palm oil mill Industry.

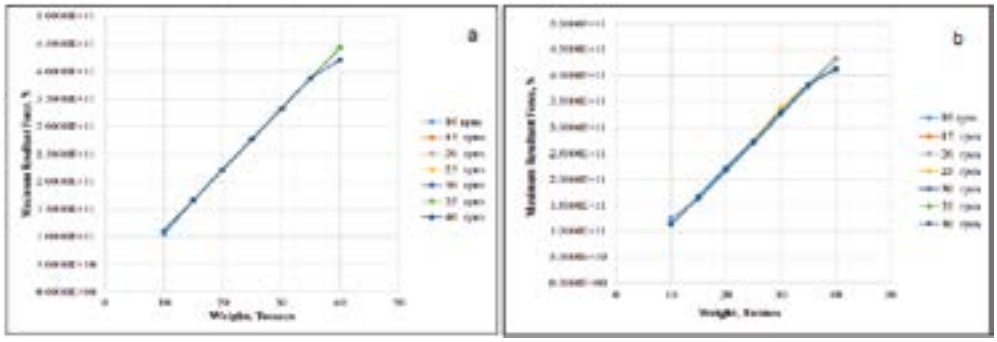

Figure 2. (a) Graph of Dura Varieties using Structural Steel (b) Graph of Tenera Varieties using Structural Steel

Acknowledgement: This work is part of the Special Short Term Grant with grant number F02/SpSTG/1387/16/29, rendered by the Universiti Malaysia Sarawak.

References:

[1] Balu Nambiappan; Azman Ismail,Norfadilah Hashim,Nazlin Ismail,Dayang Nazrima Shahari;Nik Abdullah Nik Idris, Noraida Omar,Kamalrudin Mohamed Salleh,Nur Ain Mohd Hassan and Kushair.(2018).Malaysia: 100 Years of Resilient Palm Oil Economic Performance Vol. 30 .March 2018.p.13-25. DOI:https://doi.org/10.21894/jopr.2018.0014

[2] Olaoye, J.O., Oni, K.C. and Olaoye, M.O. (2011). Computer applications for selecting operating parameters in a stationary grain crop thresher. Journal of Agricultural Technonogy 7(1): 39-56.

INNOVATION TECHNOLOGY EXPO
(INTEX) 2018 CONFERENCE
Kuching, Sarawak, Malaysia, July 17-18, 2018

BEC-2018-07

Effect of Surfactants to The Electrical Properties of the Hole Transporting Layer of Organic Solar Cells

Nur Tahirah Razali[1,*], Dominic Sanchez Merom[1], Marini Sawawi[1], Magdalene Andrew Munot[1], Shahrol Mohamaddan[1], Mahshuri Yusof[1] and Siti Kudnie Sahari[1]

[1] Department of Mechanical and Manufacturing Engineering, Faculty of Engineering, Universiti Malaysia Sarawak.
* (E-mail: rntahirah@unimas.my)

A study to identify the effect of surfactant to conductivity of the hole transporting layer (HTL) solution of organic solar cells (OSC) was conducted. Ethylene glycol, sorbitol and dimethyl sulfoxide (DMSO) are the frequently used surfactants to increase the HTL conductivity,[1]–[3] while Triton X-100 is a surfactant that is mainly used to wet the HTL solution on other organic layers surfaces.[1], [4] Therefore, the conductivity of HTL added with Triton X-100 at different concentrations was conducted and compared to that of the added DMSO.

Poly(3,4-ethylenedioxythiophene): poly (styrene sulfonate) (PEDOT: PSS) Clevios PH100 from Heraus was used as the HTL solution. Both DMSO and Triton X-100 were purchased from Sigma Aldrich. PEDOT: PSS solution with 1.0 wt% and 2.0 wt% of different surfactants were prepared separately. Pristine PEDOT: PSS solution was also prepared as a control solution. The solutions were stirred for 5 hours before spin coated on the cleaned glass substrates at 1000 rpm for 60 seconds. Then, the substrates were heated at 200°C for 10 minutes. Two probe method with Keithley 2450 source meter were used to measure the film resistivity by applying Eq.1, then converted to the conductivity by using Eq.2. Finally, the surface morphologies of the films were characterized by using Scanning Electron Microscope (SEM).

$$\rho = \frac{VA}{IL} \text{ ----------} \quad \text{Eq. (1)}$$

$$\sigma = \frac{1}{\rho} \text{ ----------} \quad \text{Eq. (2)}$$

$\rho = resistivity\ (\Omega m)$ $V = voltage\ (V)$ $I = current\ (A)$
$L = length\ (m)$ $\sigma = conductivity\ (S/m)$

Based on our findings, we can conclude that by increasing the Triton X-100 and DMSO concentration to the PEDOT: PSS solution lead to higher conductivity (Figure 1).

Triton shows that it can act both as wetting surfactant as well as improves the PEDOT: PSS conductivity which will lead to a higher power conversion efficiency of OSC although DMSO shows higher concentration than Triton X-100. Surface morphologies of PEDOT: PSS films with different DMSO concentration exhibit similar surface condition probably due to low concentration of the surfactant.

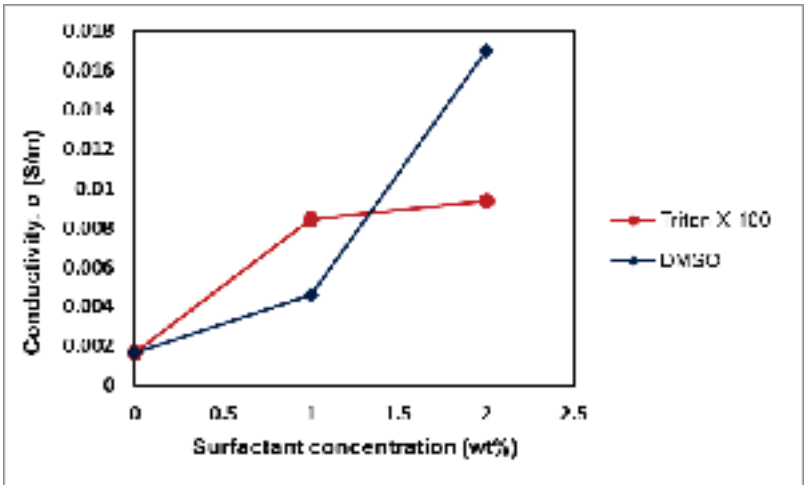

Figure 1. Conductivity of PEDOT: PSS films with different concentration of Triton X-100 and DMSO.

Acknowledgment: The work was supported by UNIMAS Special Short Term Grant (SpSTG), grant number F02/SpSTG/1379/16/21.

References:

[1] C. Zhang, Y. Zhang, H. Guo, Z. Zhang, and C. Zhang, "Hole-Transporting Layer Treatment of Planar Hybrid n-Si/PEDOT:PSS Solar Cells with Power Conversion Efficiency up to 14.5%," *Int. J. Photoenergy*, vol. 2017, 2017.

[2] A. M. Nardes, M. Kemerink, M. M. de Kok, E. Vinken, K. Maturova, and R. A. J. Janssen, "Conductivity, work function, and environmental stability of PEDOT:PSS thin films treated with sorbitol," *Org. Electron. physics, Mater. Appl.*, vol. 9, no. 5, pp. 727–734, 2008.

[3] R. Nagata, Y. Yanagi, S. Fujii, H. Kataura, Y. Nishioka, and Ieee, "Application of Highly Conductive DMSO-Treated PEDOT:PSS Electrodes to Flexible Organic Solar Cells," *2014 21st Int. Work. Act. Flatpanel Displays Devices*, pp. 299–302, 2014.

[4] N. T. Razali, I. Osaka, K. Takimiya, V. Vohra, and H. Murata, "Achieving high efficiency and stability in inverted organic solar cells fabricated by laminated gold leaf as top electrodes," *Appl. Phys. Express*, vol. 7, no. 11, p. 111602, 2014.

INNOVATION TECHNOLOGY EXPO
(INTEX) 2018 CONFERENCE
Kuching, Sarawak, Malaysia, July 17-18, 2018

BEC-2018-08

Conceptual Design and Analysis of Sago Drying Machine

Shahrol Mohamaddan[1,*], Hao Xian Lew[1], Mohd Fadzli Ashari[1], Marini Sawawi[1] and Mohamad Syazwan Zafwan Mohamad Suffian[1]

[1] Department of Mechanical and Manufacturing Engineering, Faculty of Engineering, Universiti Malaysia Sarawak.
* (E-mail: mshahrol@unimas.my)

The increasing demand of sago flour in various areas mainly the food industry indicates the need to enhance the productivity of sago. Sago is a powdery starch which is extracted from the pith inside the trunk of sago palm called Metoxylon Sagu. Metroxylon is derived from the Greek word meaning heart wood. Sago is a primary staple food for the lowland people such in New Guinea and the Moluccas [1]. The people tend to cook and eat the sago in the form of pan cake with fish. In Malaysia, sago is inexpensive and reliable source of starch although it is not a staple food [2]. Sago palm has the highest production among the starchy crop and it has been named as the 'starch crop of 21st century' [3]. One sago palm is able to yield around 150 to 300 kg of sago.

In conventional sago mill, the most economic method to dry the sago is wood-fired technique which including the burning of wood [4]. Unfortunately, the inefficient usage of wood fired dehydrator and the greenhouse gas emission are degrading the environment. For solar drying, the method is time consuming and subjected to weather constraint especially when cloudy and rainy day. For hot air drying, the process takes longer time to be completed. For example, under 50-60°C the process takes 90-120 minutes to decrease the moisture content in tapioca sago from 40% to 10%. It is also found that the tapioca moisture content drop from 30% to 10% in 60 minutes at 30-35°C [5].

In this research, conceptual design of new sago drying machine is developed to support the sago industry by providing solution for drying process. The machine consists of three main components namely the tray, mixer and support area as shown in Figure 1. Before the fabrication is conducted, the mathematical modelling and simulation analysis is conducted to verity the new design. In this paper, the analysis of new sago drying machine is discussed. The analysis includes power transmission, tray bending, support bending, mixer vibration and shaft analysis. The analysis shows that the design can be operated theoretically. The general dimension and material selection for the drying machine is shown in Table 1.

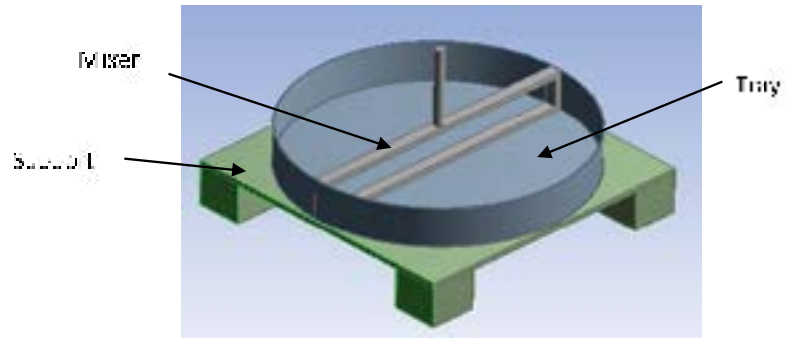

Figure 1. Conceptual design of new sago drying machine

Table 1. General dimension and material selection of sago drying machine

Subassembly	General Dimension	Material
Tray	20cm height x 90cm diameter Thickness 1mm	Stainless steel (standard part)
Support	100cm x 100cm x 20cm	Mild steel (standard part)
Mixer	20cm height x 85cm long	Stainless steel (standard part)
Dryer Chamber	110cm x 110cm x 150cm	Polycarbonate, Polyethylene

Acknowledgment: This research is supported by Osaka Gas in Cultural Exchange Foundation (OGFICE) Research Grant Scheme 2017/18 under research titled "Drying Process of Lemantak (Sago Powder) using an Automated Machine for Cottage Industries in Sarawak" and Research Acculturation Grant Schemes [Grant no: RAGS/TK01(4)/1318/2015(12)]. The authors would like to thank Universiti Malaysia Sarawak (UNIMAS) for providing facilities for this research.

References:

[1] Vijay, M., Vimalraj, S., Vinith, S., Vincent, K.V., and Vijaymohan, P. (2017). Energy efficient solar dryer for sago industries. *Int. J. Innov. Sci. Res.*, vol. 30, no. 3, 493–500.

[2] Mazlina, S., Kamal, M., Mahmud, S.N., Hussain, S.A. and Ahmadun, F.R. (2007). Improvement on sago flour processing. *Int. J. Eng. Technol.*, vol. 4, no. 1, 8–14.

[3] Mustafa Kamal, M., *et al.*(2017). Effect of temperature to the properties of sago starch. *IOP Conference Series: Materials Science and Engineering*, vol. 206, p. 012039.

[4] Pendita, A., Lim, P.Y., and Junis, H.V.H. (2014). Development and experimental studies of a small-scaled solar-powered sago plant dehydrator. *Int. J. Adv. Sci. Eng. Inf. Technol.*, vol. 4, no. 5, 52–55.

[5] Pandian, P.S. and Meenambal, T. (2017). Studies on performance of recent techniques adopted in various starch and sago industries. *Int. J. Eng. Technol.*, vol. 7, no. 7, 122–129.

INNOVATION TECHNOLOGY EXPO
(INTEX) 2018 CONFERENCE
Kuching, Sarawak, Malaysia, July 17-18, 2018

BEC-2018-09

Effect of Fibre (Polypropylene) Volume in Mortar Mixed with POFA

Raudhah Ahmadi[1,*], Dora Ediba Lucas[1], Emellis Machillies[1], Mohd Syukry Saiful[1], Md Abdul Mannan[1] and Idawati Ismail[1]

[1] Department of Civil Engineering, Faculty of Engineering, Universiti Malaysia Sarawak.
* (E-mail: araudhah@unimas.my)

It is envisaged that high strength fibre reinforced concrete could exhibit high compressive and tensile strength under loadings. This paper is intended to assess the effect of fibre (polypropylene) volume inclusion in mortar mixed with Palm Oil Fuel Ash (POFA). Experimental studies are carried out as tabulated in Table 1 to assess the mechanical behavior of fibre reinforced mortar and comparing them with normal concrete. Compressive strength and split tensile tests are conducted in this study. In the experiments, the aspect ratio of fibre (polypropylene) volume inclusion is fixed to 33. An optimum volume of 40% microfine POFA (1-10μm) is included as partial cement replacement. POFA is initially burned up to 500°C for 90 minutes to eliminate excess carbon and moisture.

Table 1. Mortar samples for mechanical tests

Samples	OPC	POFA	Fibre
A	100%	-	-
B	100%	-	10 kg/m3
C	100%	-	15 kg/m3
D	100%	-	20 kg/m3
E	60%	40%	-
F	60%	40%	10 kg/m3
G	60%	40%	15 kg/m3
H	60%	40%	20 kg/m3

It can be observed from Figure 1 that mortar mixed with POFA has slower early strength compared to mortar that contains 100% OPC. This is due to the fact that there was a prolong hydration process of POFA. Lower cement content in the mix and pozzolanic behaviour were the main cause for reducing heat of hydration in concrete that contains POFA. The effect of fibre dosage inclusion on compressive strength can be seen in Figure 1. As can be observed in the inclusion of 10 kg/m^3 polypropylene fibre, there is increase in the compressive strength 80.5 Mpa (100% OPC-56 days) and 79.5Mpa (40% POFA as partial cement replacement-56 days). The increase in compressive reading for 10 kg/m^3 fibre

inclusion may be due to transverse confinement effect of polypropylene fibre that restrained the lateral expansion of mortar cube samples [1]. Inclusion of fibre may aid in arresting the development of microcracks which leads to higher value of compressive strength.

The decrease in compressive strength reading is envisaged due to increase in voids and perturbation of matrix. In addition to the fibre quantity, perturbation also depends on the ability of matrix to accommodate fibre [2]. Therefore, addition of fibre is a balancing between microcracks bridging and additional voids that is caused by fibre addition. In this study, the optimum fibre dosage inclusion is 20 kg/m^3 that exhibit 82.4Mpa and 78.7 MPa stresses at 56 days of curing for both 100% OPC and 40%POFA inclusion samples, respectively.

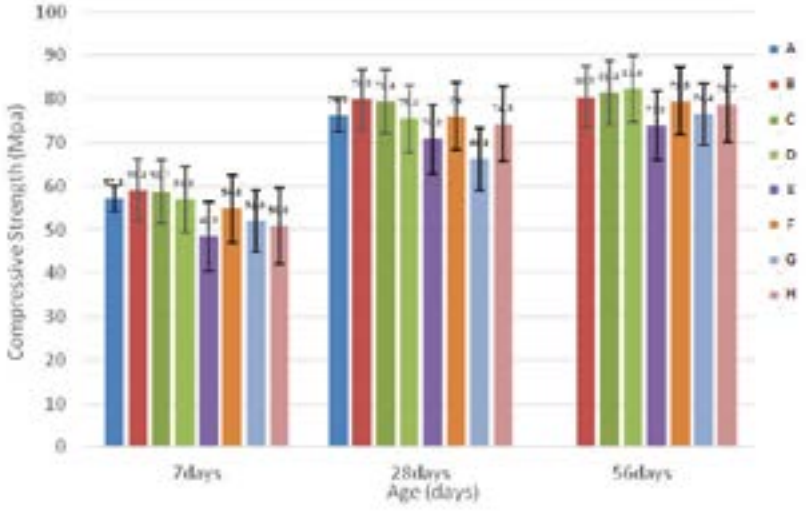

Figure 1: Average Compressive Strength of Samples as tabulated in Table 1 at the 7th, 28th and 56thdays of water curing.

Results from split tensile strength test show that mix that contain 40% ultrafine POFA as partial cement replacement mixed with 10kg/m^3 of polypropylene fibre has the highest average reading of tensile strength at 28 days of curing, 6.6 MPa. Inclusion of fibre in mortar sample helps to increase the flexural strength as well as bridging the crack propagation in mortar sample. Too much fibre addition in mortar sample slowly degrading the tensile strength of mortar.

Acknowledgment: This project was funded by OSAKA Gas in Cultural Exchange Foundation (OGFICE) Research Grant Scheme 2017/2018 rendered by the Universiti Malaysia Sarawak.

References:

[1] Lee, S., Oh, J., & Cho, J. (2015). Compressive Behavior of Fiber-Reinforced Concrete with End-Hooked Steel Fibers. *Materials.*1442–1458. ISSN 1996-1944

[2] Neves, R. D., & Almeida, J. C. O. F. De. (2005). Compressive behaviour of steel fibre reinforced concrete. *Structural Concrete*.6, No.1

INNOVATION TECHNOLOGY EXPO
(INTEX) 2018 CONFERENCE
Kuching, Sarawak, Malaysia, July 17-18, 2018

BEC-2018-10

Fabrication and Mechanical Properties of Cellulose Nanofiber Reinforced Polyvinyl Alcohol Composites

Noor Hisyam Noor Mohamed[1,*], Sinin Hamdan[1], Marini Sawawi[1], Mahsuri Yusof[1] and Md Rezaur Rahman[1]

[1] Department of Mechanical and Manufacturing Engineering, Faculty of Engineering, Universiti Malaysia Sarawak.
* (E-mail: nmnhisyam@unimas.my)

Polyvinyl alcohol (PVA) is a biodegradable polymer with excellent mechanical properties, non–toxic, good film-forming ability and water soluble. Cellulose nanofiber (CNF) has a potential as reinforcement material with PVA as CNF showing good mechanical properties, organic and abundant in nature.

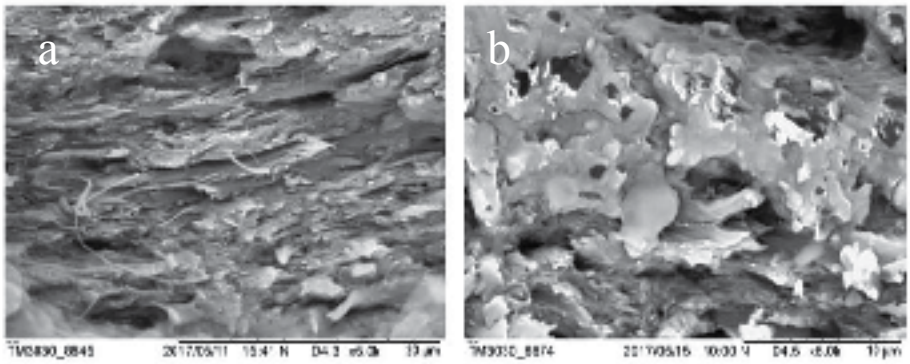

Figure 1. SEM images for untreated CNF/PVA-f 40 wt% (b) SEM images for heat treated CNF/PVA-f 40 wt%

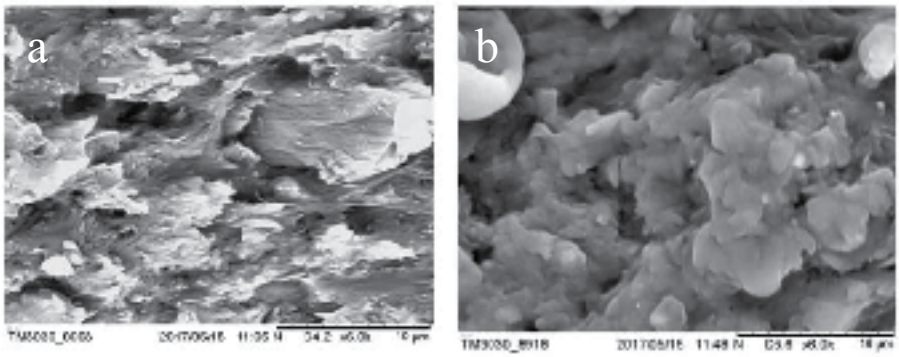

Figure 2. SEM images for untreated CNF/PVA-p 40 wt% (b) SEM images for heat treated CNF/PVA-p 40 wt%